Cell Systems, Volume *15*

Supplemental information

Stimulus-response signaling dynamics characterize macrophage polarization states

Apeksha Singh, Supriya Sen, Michael Iter, Adewunmi Adelaja, Stefanie Luecke, Xiaolu Guo, and Alexander Hoffmann

Supplemental Figure 1

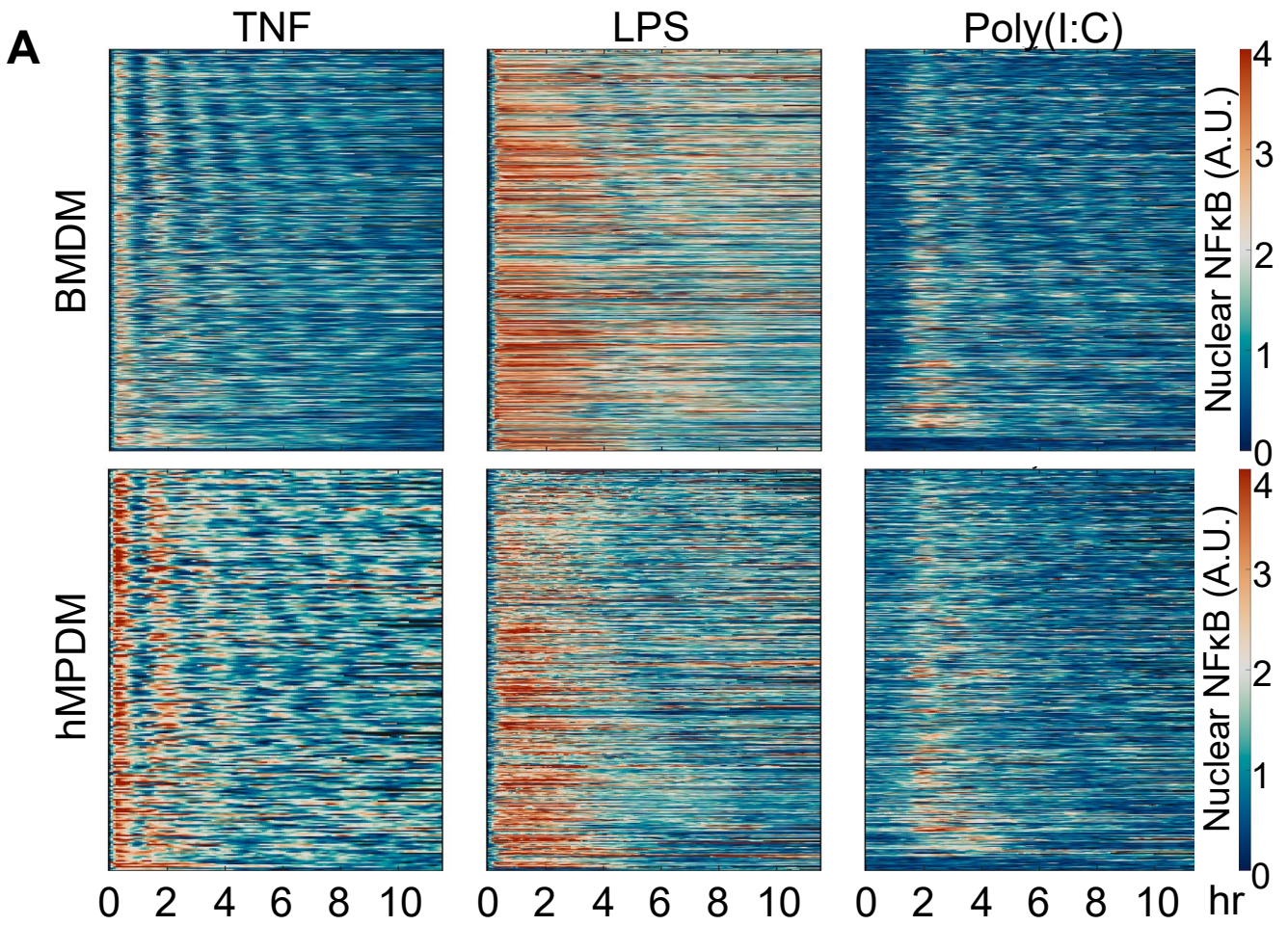

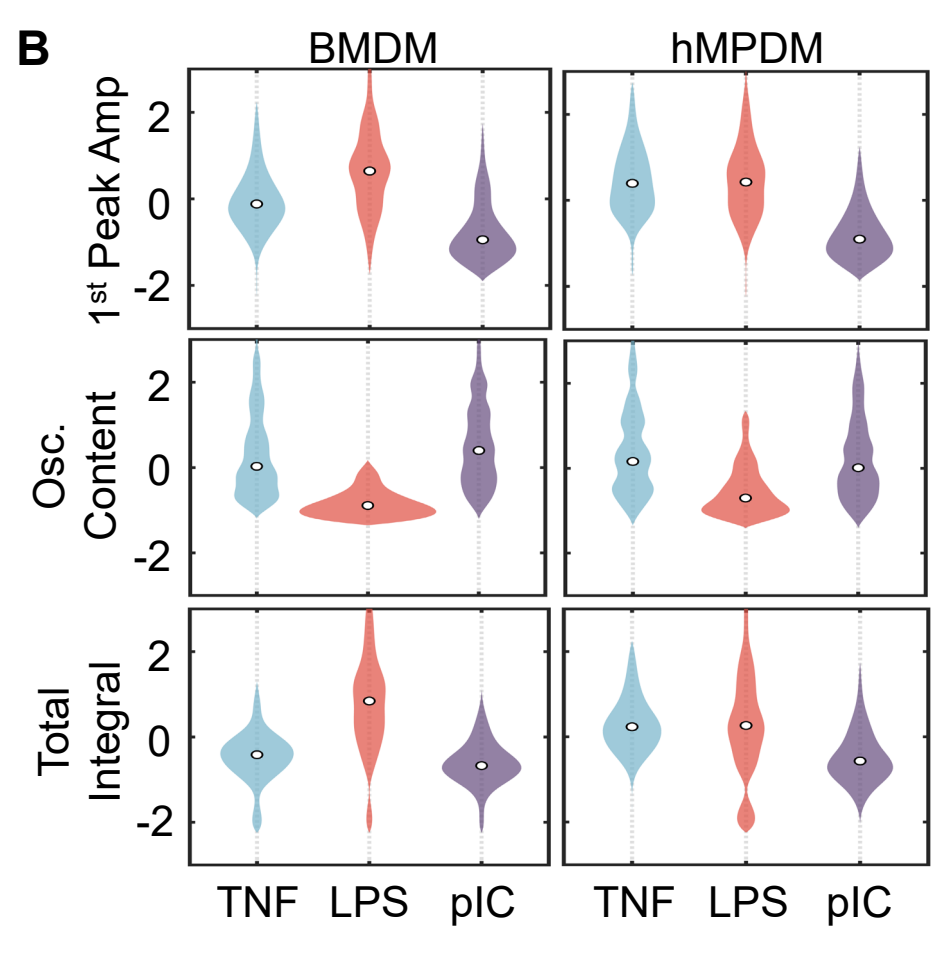

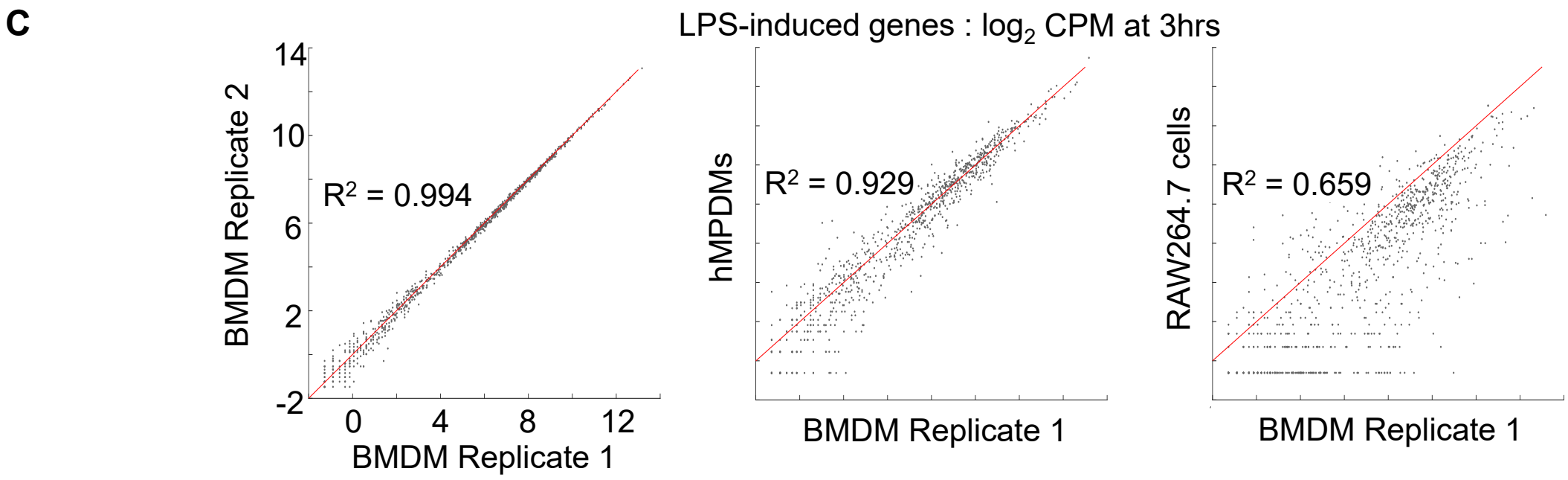

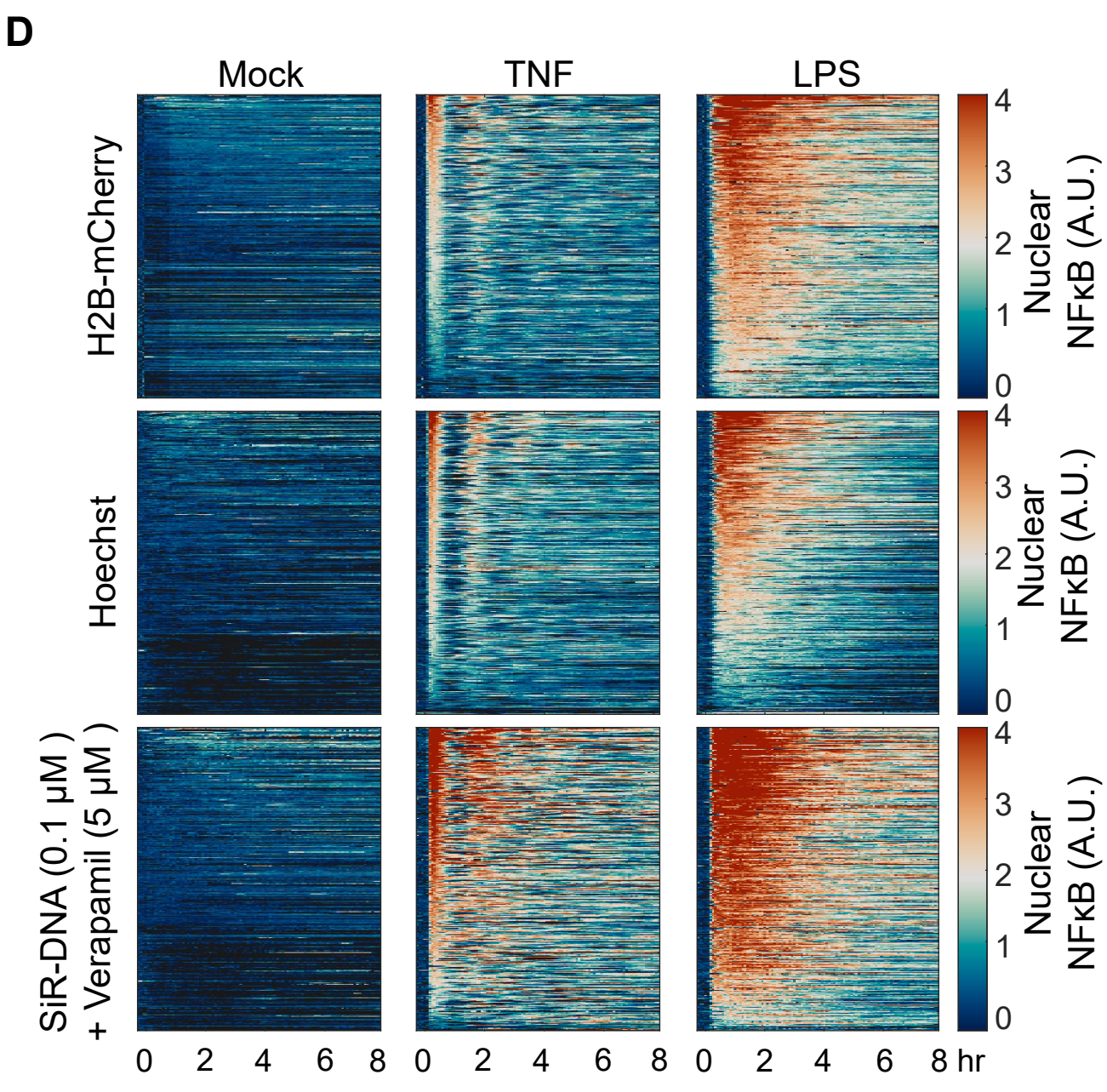

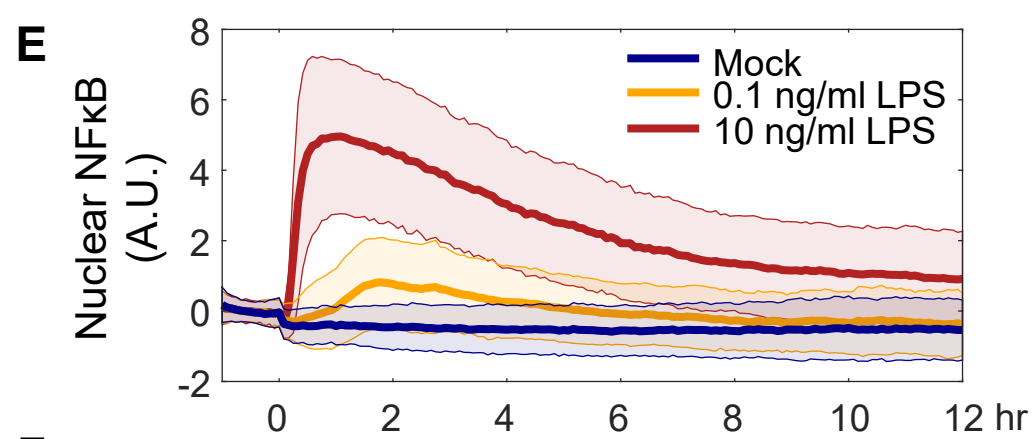

Figure S1: Controls for the imaging workflow: hMPDMs vs BMDMs, nuclear markers, photostability, related to Fig1. A. Heatmaps of single-cell NFκB trajectories in response to stimulation with TNF, LPS, and Poly(I:C) produced in BMDMs (top), and hMPDMs (bottom). **B.** Distribution of z-scored NFκB trajectory features in BMDM and hMPDM single cell responses to TNF, LPS, and Poly(I:C) stimulation. **C.** Scatterplot of $\log_2$ CPM RNA-seq data following 3 hours of LPS stimulation in BMDM, hMPDM, and RAW264.7 cells. LPS-induced genes (914 genes) are defined as having a $\log_2$ Fold Change equal to or greater than 1 compared to unstimulated basal expression in two replicates of BMDMs. **D.** Comparison of nuclear markers used for the quantitation of nuclear signals within the image-analysis pipeline. Heatmaps of hMPDM NFκB signaling dynamics in response to mock, 10 ng/ml TNF, and 10 ng/ml LPS stimulation using endogenously expressed H2B-mCherry, Hoechst dye, or SiR-DNA dye as nuclear marker. Cell trajectories are sorted by 1st peak amplitude. **E.** Little evidence of photobleaching as nuclear mVenus-RelA fluorescence declines little over 12 h after mock stimulation of hMPDMs. Mean +/- stdv of cells in one experiment (n=300-322). **F.** Little evidence of photobleaching as nuclear mVenus-RelA fluorescence shows similarly little decline over 2 h after mock stimulation with 120 (top) or 24 (bottom) images acquired within 2 hours using a 1 min or a 5 min frame rate, respectively. Mean +/- stdv of the data (n=295-479).

Supplemental Figure 2

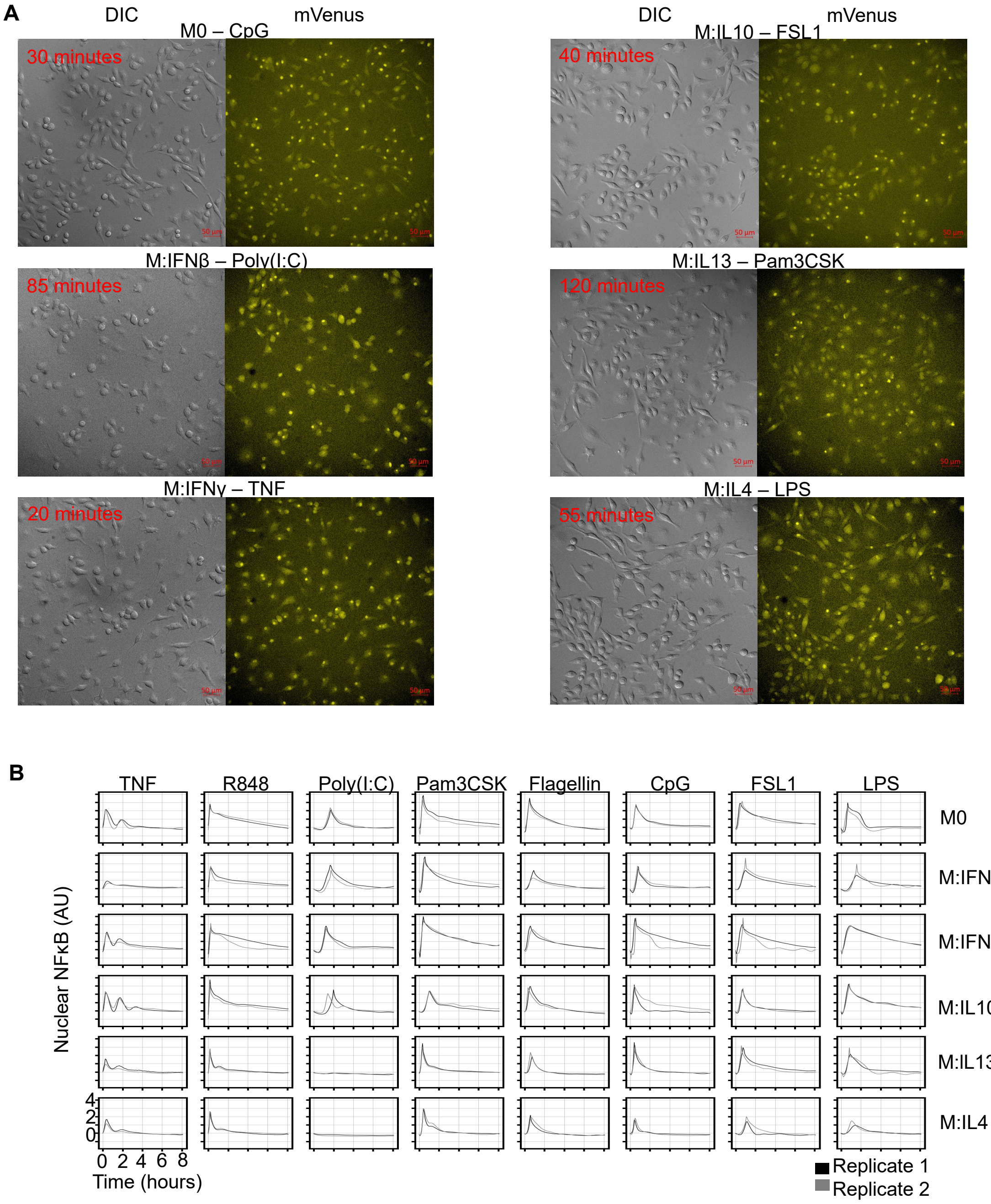

Figure S2: Example live cell microscopy images and overview of experimental single-cell NFκB trajectories, related to Fig1 A. Representative brightfield and fluorescence microscopy images from the hMPDMs across different polarization and stimulation conditions, demonstrating mVenus-RelA localization to the nucleus following stimulation (time reported is minutes after stimulation). Scale bar denotes 50 μm. **B.** Soft-DTW (dynamic time warping) barycenter of all NFκB trajectories in each replicate for all experimental conditions (computed using softdtw_barycenter from the tslearn package with smoothing hyperparameter γ = 5). A barycenter is a constructed trajectory that minimizes the pairwise distance between itself and each trajectory in the input dataset and the soft-DTW implementation offers a differentiable loss function that as consequence introduces a smoothing hyperparameter. We visualized the DTW barycenter rather than the simple timepoint-wise mean of the trajectories, since the former accounts for temporal displacement of dynamical patterns, while the latter can obscure these patterns, such as oscillations. In this aggregate form NFκB dynamics showed stimulus-specificity, with notable TNF-induced oscillations for example, as well as a degree of polarization specificity, such as a loss in response to Poly(I:C) with IL13 and IL4 polarization.

Supplemental Figure 3

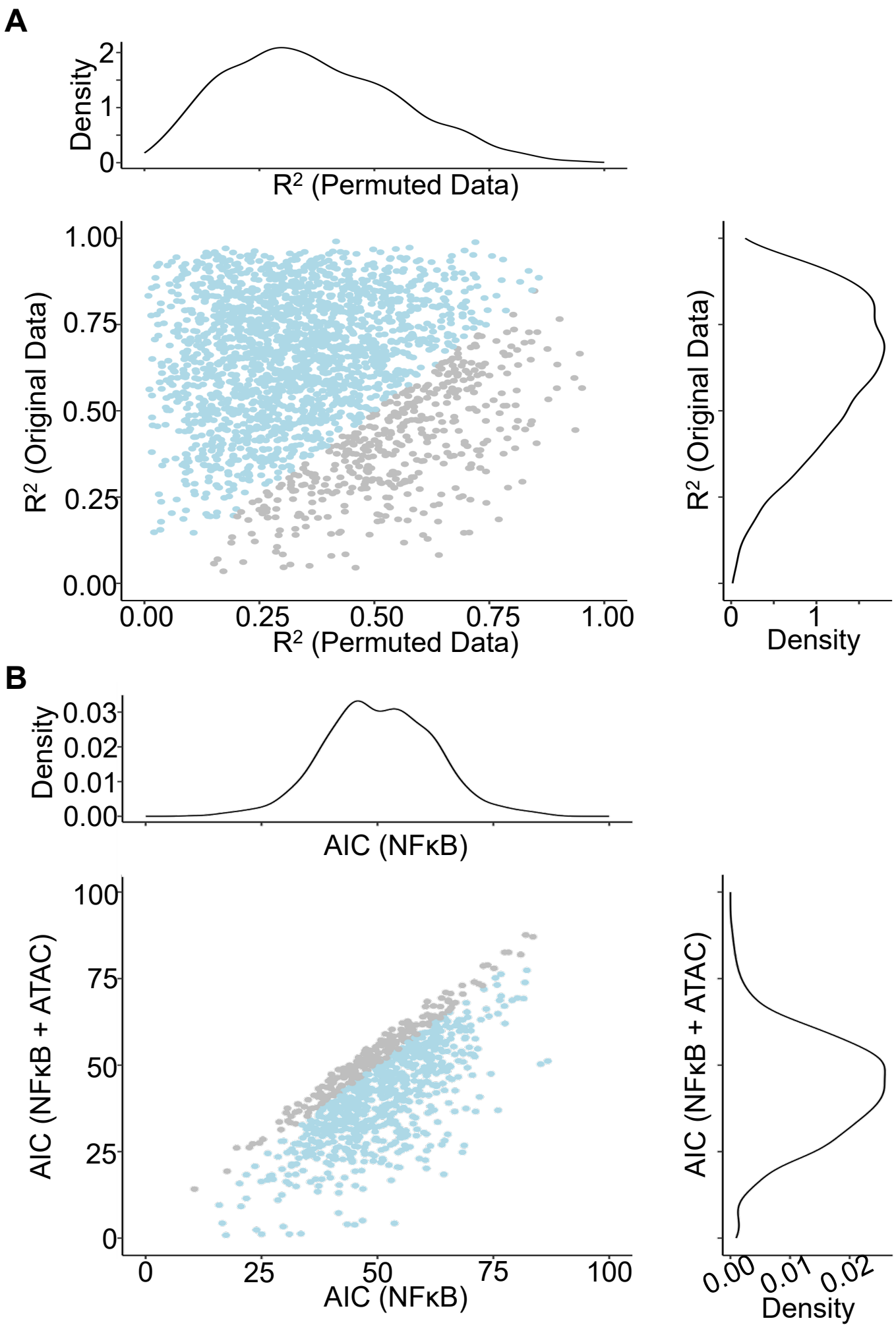

Figure S3: NFκB signaling dynamics can inform differential gene expression with polarization, related to Fig1. A. R^2 values from fitting a linear model to average NFκB total activity to predict gene expression in naïve, IFNβ, and IFNγ conditioned human macrophages displayed versus R^2 values from fits to permuted gene expression data. For 81% of the 2299 genes interrogated, the R^2 value for the model based on the original data exceeded the R^2 value for the model based on the permuted data, suggesting the NFκB signaling dynamics can indeed carry information about differences in gene expression related to polarization state. However, the average R^2 value for these models across all genes was only 0.62. **B.** AIC of the linear models fit only to average NFκB total activity to predict gene expression displayed versus AIC of linear models fit to both average NFκB total activity and average chromatin accessibility (ATAC) in the promoter region for a subset of 947 genes that had some peaks identified ± 1 kilobases from the transcription start site. For 75% of the genes, the AIC value for model based on both NFκB total activity and promoter chromatin accessibility was less than that for the model based only on NFκB total activity, suggesting that chromatin accessibility can add information to NFκB signaling dynamics to better inform differences in gene expression related to polarization state.

Supplemental Figure 4

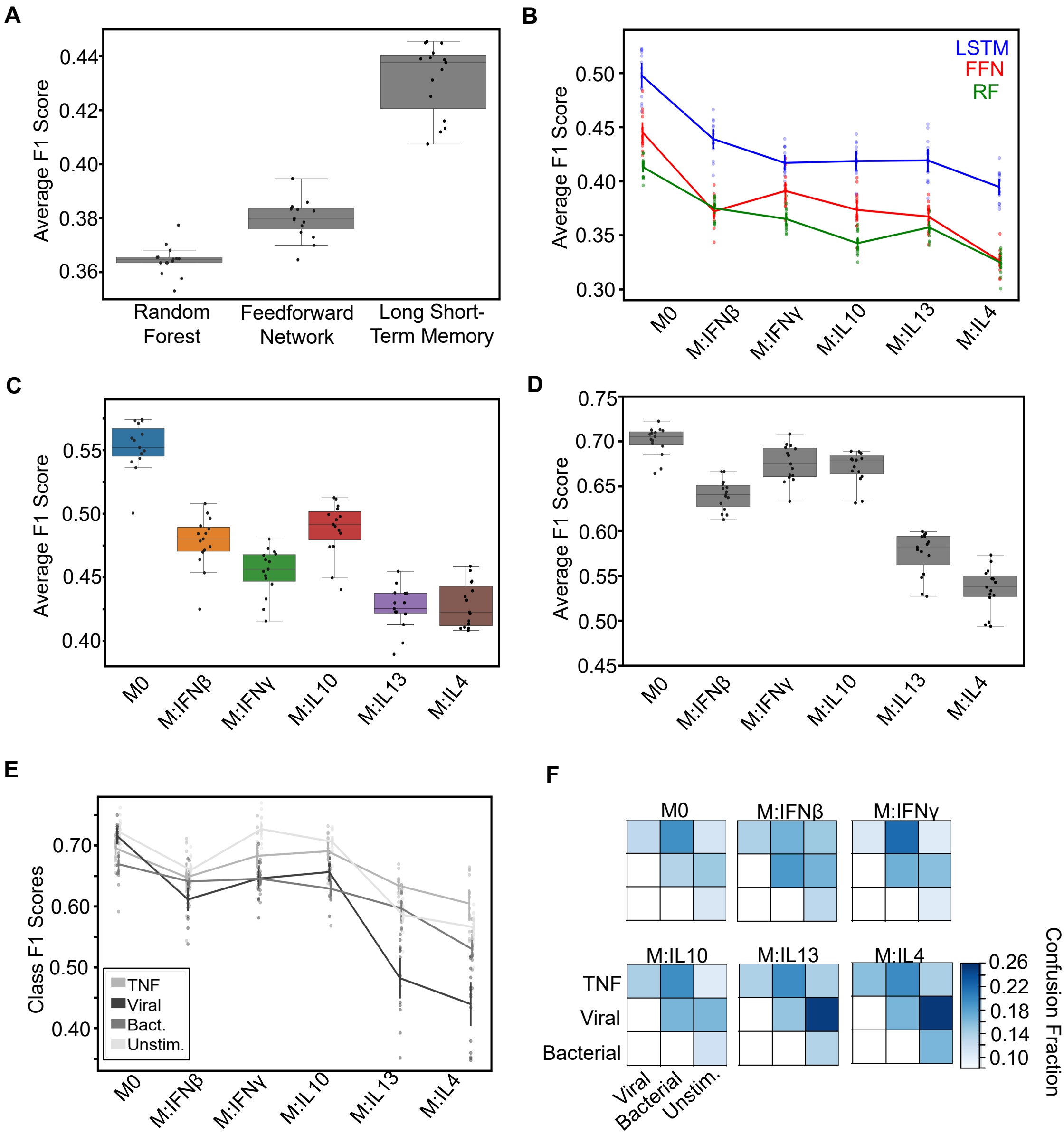

Figure S4: Evaluation of LSTM-based ML classifier performance, related to Fig2 A. Comparison of the macro-averaged F1 scores for the task of identifying each ligand (including unstimulated) from the time series data across all polarization conditions using Random Forest, Feedforward Network, and LSTM-based classifier models. **B.** Macro-averaged class F1 scores for the task of classifying each ligand individually across all polarization states reveal overall loss of specificity with polarization for the LSTM, Feedforward Network (FFN), and Random Forest (RF) classifier models. **C.** Macro-averaged class F1 scores for the task of classifying each ligand individually (including unstimulated) with a LSTM-based model trained separately for each polarization state again reveals overall loss of specificity with polarization. **D.** Macro-averaged class F1 scores for the task of classifying each ligand source (host TNF, viral, bacterial, and unstimulated) across polarization states demonstrates loss of stimulus response specificity with polarization. 3427 cells were sampled from each condition for this classification task. **E.** Average class F1 scores across polarization states shows greatest loss in viral distinguishability with polarization **F.** Average confusion fractions across polarization states for different ligand sources illustrates common trends with polarization, such as increased viral vs bacterial confusion, as well as polarization specific changes such as increased viral vs unstimulated confusion with IL13 and IL4 conditioning. Error bars in B and E correspond to 95% confidence intervals with n=15.

Supplemental Figure 5

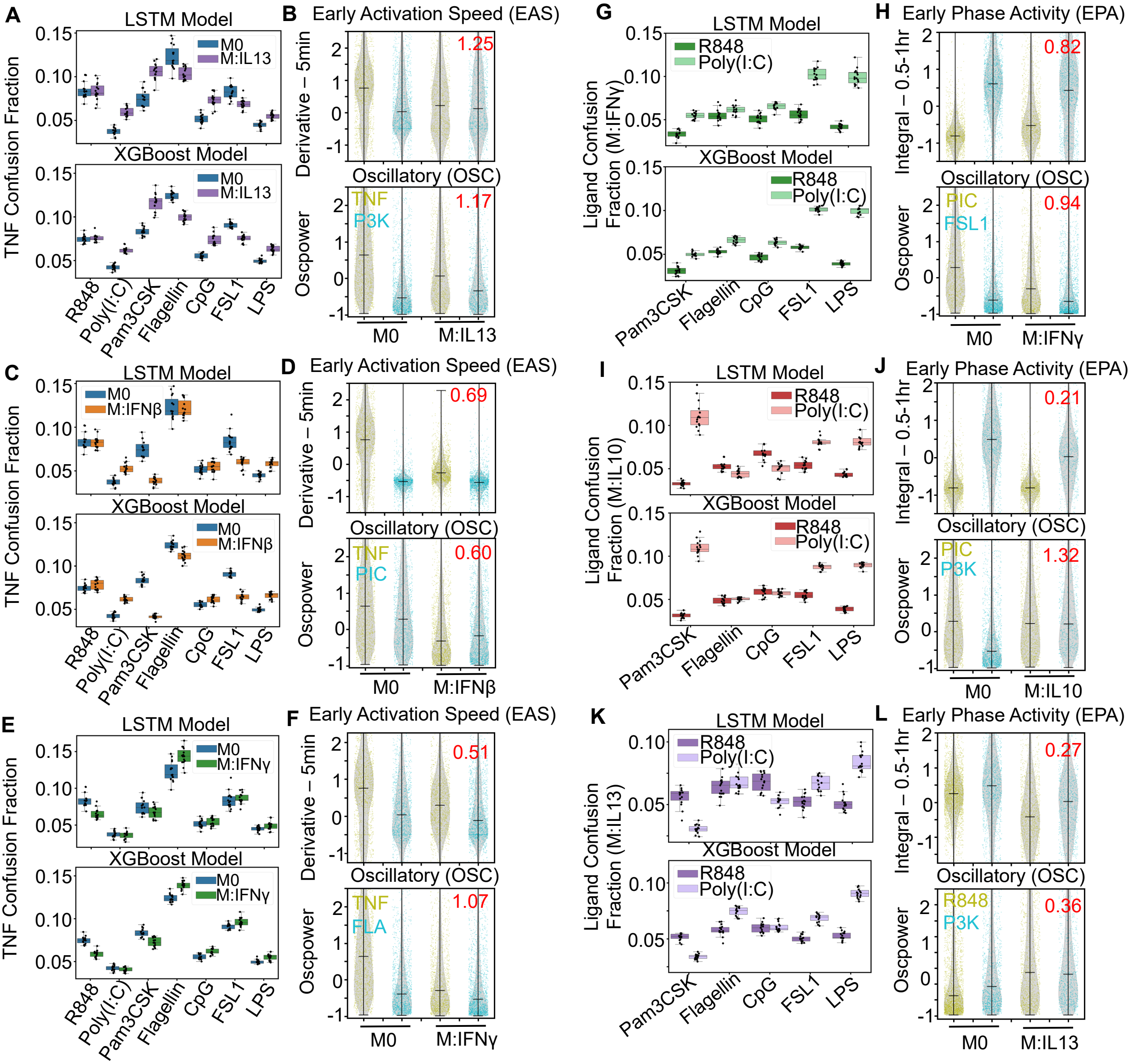

Figure S5: Examples of increased host TNF and pathogen confusion and convergence of viral and bacterial responses with polarization, related to Fig5 **A.** Confusion fractions derived from both the LSTM and XGBoost models between the host ligand (TNF) and the pathogen ligands (R848, Poly(I:C), Pam3CSK, Flagellin, CpG, FSL1, LPS) in the M0 and IL13 polarization states shows larger increase with Poly(I:C), Pam3CSK, CpG, and LPS stimulation. **B.** Feature distributions from the single-cell responses to TNF and Pam3CSK (P3K) with M0 and IL13 polarization reveal decreased early activation speed and oscillations of TNF contribute to convergence; log2 fold reduction in Jensen-Shannon Distance between ligand responses with polarization in red. **C.** Confusion fractions between TNF and the pathogen ligands in the M0 and INFβ polarization states shows larger increase with Poly(I:C) and LPS stimulation. **D.** Feature distributions from the single-cell responses to TNF and Poly(I:C) (PIC) with M0 and INFβ polarization reveal decreased early activation speed and oscillations of TNF responses with INFβ polarization contribute to convergence **E.** Confusion fractions between TNF and the pathogen ligands in the M0 and INFγ polarization states shows larger increase with Flagellin stimulation. **F.** Feature distributions from the single-cell responses to TNF and Flagellin (FLA) with M0 and INFγ polarization reveal decreased early activation speed and oscillations of TNF responses with INFγ polarization contribute to convergence. **G.** Confusion fractions between the viral ligands (R848, Poly(I:C)) and the bacterial ligands (Pam3CSK, Flagellin, CpG, FSL1, LPS) in the IFNγ polarization state shows greatest confusion with Poly(I:C) and FSL1 stimulation. **H.** Feature distributions from the single-cell responses to Poly(I:C) and FSL1 with M0 and IFNγ polarization reveal increased early phase activity and decreased oscillations of Poly(I:C) responses with IFNγ polarization contribute to convergence. **I.** Confusion fractions between the viral and bacterial ligands in the IL10 polarization state shows greatest confusion with Poly(I:C) and Pam3CSK stimulation. **J.** Feature distributions from the single-cell responses to Poly(I:C) and Pam3CSK with M0 and IL10 polarization reveal decreased early phase activity and increased oscillations of Pam3CSK responses with IL10 polarization contribute to convergence **K.** Confusion fractions between the viral and bacterial ligands in the IL13 polarization state shows greatest confusion of Pam3CSK with R848 stimulation. **L.** Feature distributions from the single-cell responses to R848 and Pam3CSK with M0 and IL13 polarization reveal decreased early phase activity and increased oscillation for both stimuli responses with IL13 polarization contribute to convergence.

Supplemental Figure 6

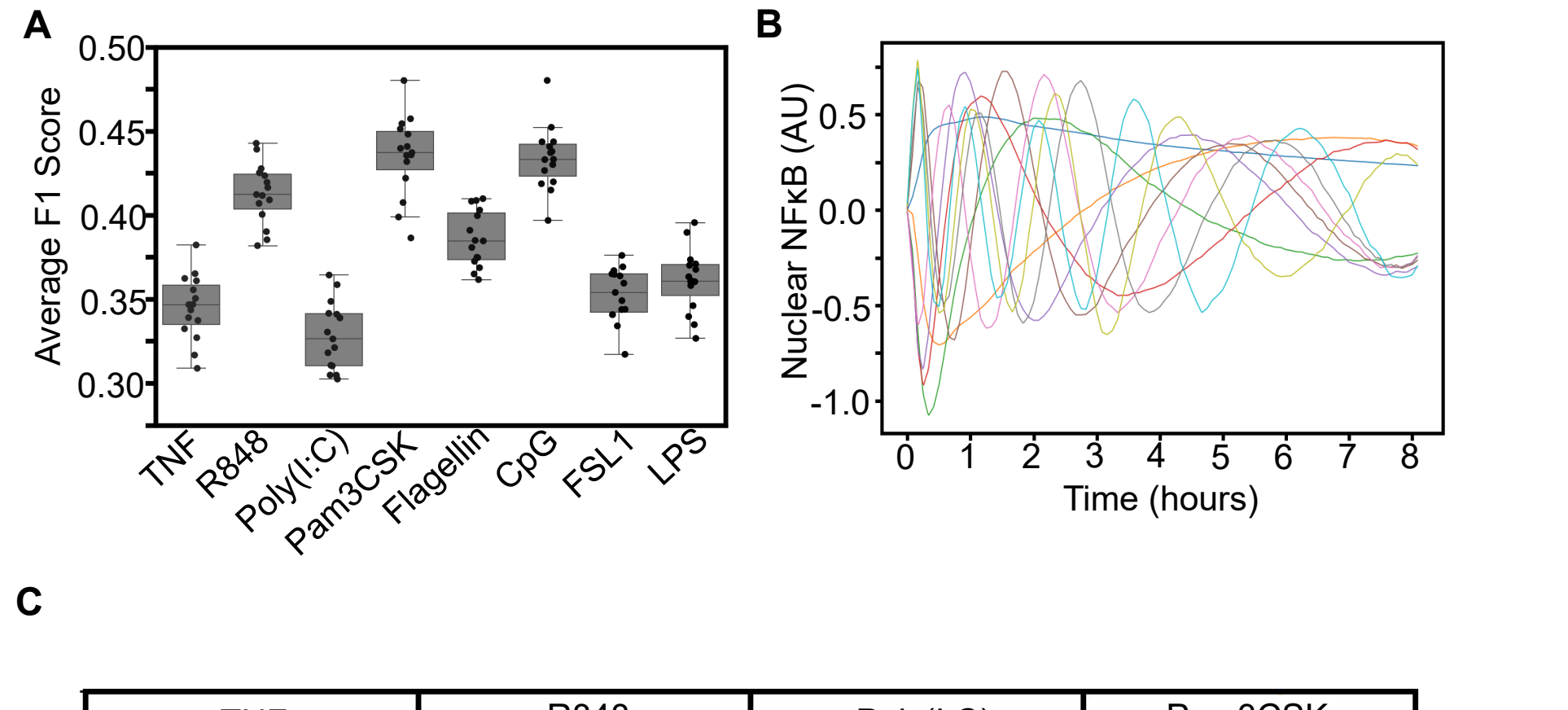

Figure S6: Mapping macrophage polarization states with NFκB signaling response time series data, related to Fig6. **A.** Macro-averaged class F1 scores from the LSTM classifier for the task of classifying each polarization condition across stimulation conditions provides a quantification of polarizer distinguishability across the stimuli. **B.** First 10 principal components identified by functional PCA (capturing approximately 85.39% of the variance) used as input for the UMAP projection. **C.** UMAP projection of the first 10 functional principal components of the NFκB responses for each stimulus colored by polarization state (sampled such that number of cells per condition equivalent, 1338).

Supplemental Figure 7

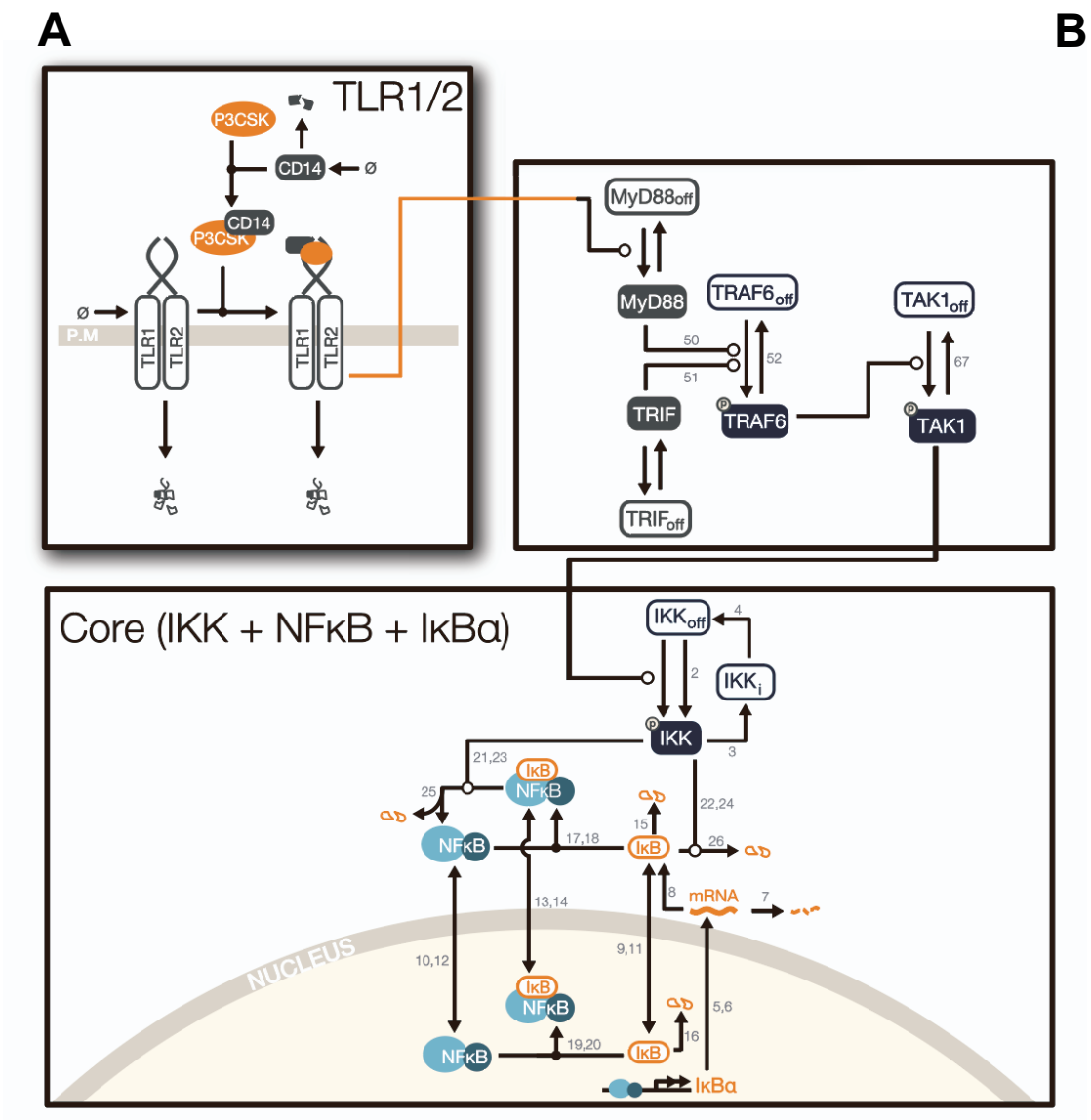

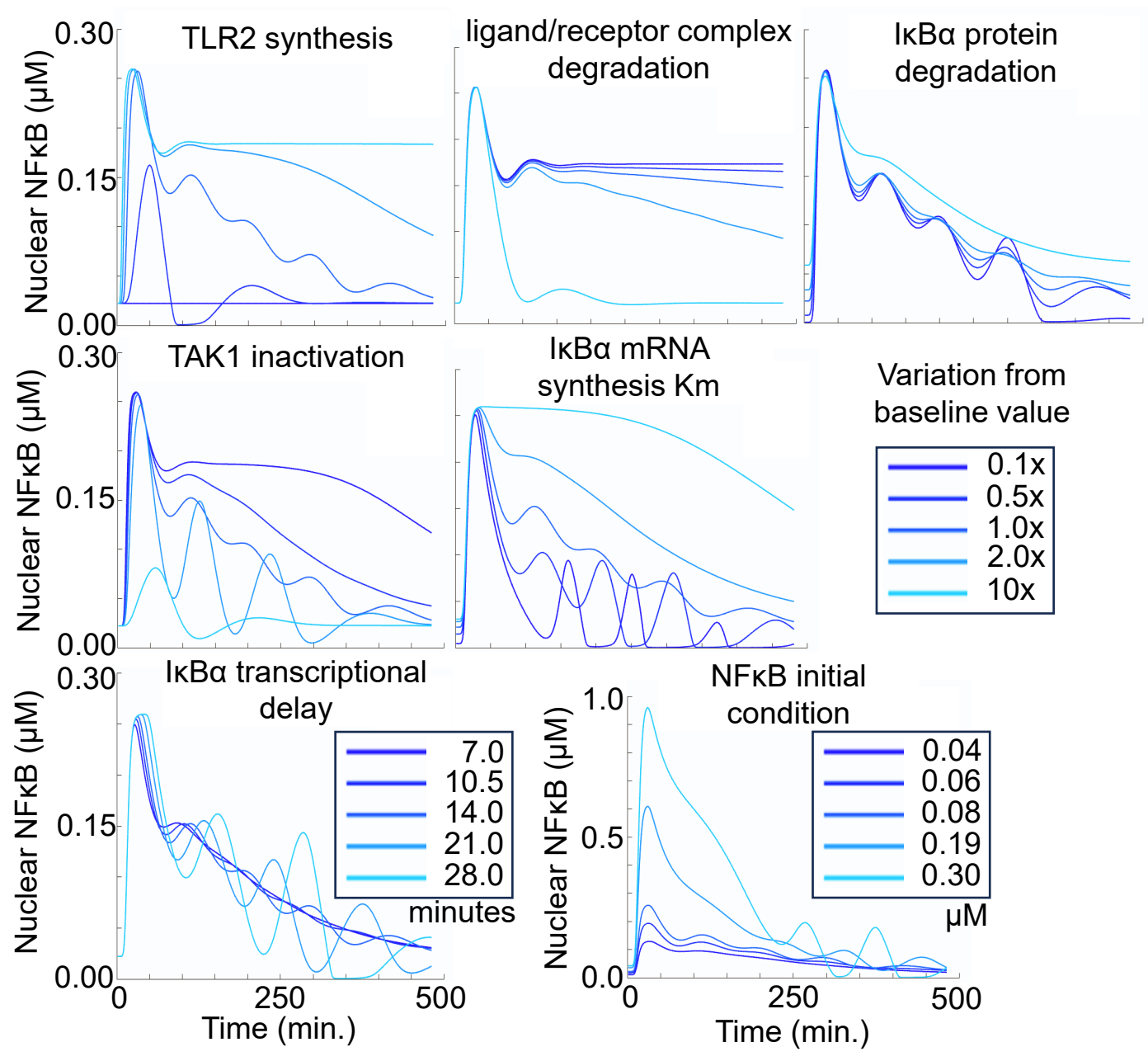

Figure S7: Mechanistic modeling of NFκB signaling pathway following TLR1/2 activation and fit biochemical parameter distributions, related to Fig7. A. Model topology (adapted from Adelaja et al., 2021) representing biochemical reactions that connect Pam3CSK binding to TLR1/2 at the cell membrane surface to NFκB nuclear translocation. These reactions are described in terms of a system of ordinary differential equations (ODE). **B.** Model simulations in which the named parameter is varied below and above its published baseline values. Varying these 7 parameters within their respective constraint regions demonstrate the sensitivity of these parameters on the resulting activation of NFκB, and hence these 7 parameters were distributed for model fitting to experimental data. **C.** Distribution of parameter values corresponding to top 10 model fits for each of the 300 cells sampled from each polarization state, revealing potential differences in the NFκB signaling network between polarization states. **D.** Single cell RNA sequencing data from Sheu et al. 2023 demonstrating changes in baseline TLR2 gene expression with macrophage polarization consistent with the fit parameter distributions for TLR2 synthesis.

Table S1: Number of Single Cell NFκB Trajectories per Replicate in each Experimental Condition (Polarization x Stimulus)

	Host	Viral		Bacterial				
	TNF	R848	Poly(I:C)	Pam3CSK	Flagellin	CpG	FSL1	LPS
M0	850	1064	882	752	737	1158	1048	873
	752	1626	512	742	795	830	864	891
M1 IFNβ	732	897	896	352	733	975	508	666
	870	576	785	512	367	690	402	451
M1 IFNγ	565	1317	744	381	961	751	1103	1116
	912	1356	579	598	786	718	665	788
M2 IL10	643	863	754	414	829	676	661	971
	1037	1078	574	344	841	372	279	818
M2 IL13	641	699	1581	476	579	556	538	746
	483	692	429	584	475	422	430	533
M2 IL4	619	669	1134	362	698	381	821	345
	650	682	744	282	356	424	362	381

Table S2: QC Metric Definitions

Duration	dur_t = time response above 0.3	n_pks = number of peaks	
EarlyVsLate	-eVl = -time to half maximum cumulative integral value		
OscVsNon	oVn = average power in 0.33 to 1 hr^{-1} frequency range		
PeakAmplitude	max_val = maximum value	pk2pk = maximum to minimum value difference	pk1_amp = amplitude of first peak
Speed	max_pk1_spd = maximum derivative value before first peak time	-pk1_t = -time to first peak	deriv2 = derivative at 10 minutes
Total	tot_act = maximum cumulative integral value		

Table S3: Trajectory Feature Library

Feature Name	Description	Included in Feature Analysis
time_series_# *(amplitude – #min)*	Value of baseline deducted NFκB fluorescence every five minutes (98 values)	time_series_1 & time_series_2 (0 & 5 minutes only)
derivatives_# *(derivative – #min)*	Central finite differences from first two hours (25 values)	yes
intwin1_#	One hour integral windows (8 values)	no
intwin3_#	Three hour integral windows (6 values)	intwin3_1 (first three hours only)
phase_diff1 *(1st vs 2nd hr integral)*	Difference between first and second hour integral windows	yes
phase_diff3	Difference between three hour window integral beginning at 0 and 3 hours	yes
intwin0_5_# *(integral – #-#+0.5hr)*	Half-hour integral windows (16 values)	yes
max_amplitude	Maximum time series value	no
min_amplitude *(min amplitude)*	Minimum time series value	yes
range *(range)*	Difference between max and min amplitude	yes
maxAmp_early *(max amplitude <2hr)*	Maximum time series value in first two hours	yes
time2Max *(time to max)*	Time to maxAmp_early	yes
timeUp2halfMax	Time to half of maxAmp_early	yes

(time to ½ max)		
timeDown2halfMax *(time to ½ max post-peak)*	Time to half of maxAmp_early after passing max	yes
peak_duration_# *(duration > #% peak)*	Number of timepoints above 50%, 70%, or 90% the max amplitude (3 values)	yes
responder_index	Responder (1) or non-responder (0) as defined by passing 3 times the baseline standard deviation for at least five consecutive frames within the first four hours	yes
off_times	Final time a cell meets the responder criteria	yes
envelope_#	Longest stretch of consecutive time above a threshold (0, 0.75, 1.5, 2.25) (4 values)	no
duration_#	time above a threshold (0, 0.75, 1.5, 2.25) (4 values)	yes
peakfreq	Peak frequency identified in power spectrum	yes
pk1_amp	Amplitude of first identified peak	no
pk1_time	Time to first identified peak	yes
pk1_width	Width (calculated at half-height of peak) of the first identified peak	yes
pk1_prom *(peak prominence)*	Prominence (over neighboring troughs) of the first identified peak	yes
max_pk1_speed *(max derivative to 1st peak)*	Maximum derivative value within time to first peak	yes
max_pk1_speed_frame	Frame at which max_pk1_speed is obtained	yes
oscpower *(oscillatory)*	Average power in 0.33-1 hr^{-1} frequency range	yes
quarter_activity	Cumulative positive activity within first quarter of time course	no
half_activity	Cumulative positive activity within first half of time course	no

total_activity	Cumulative positive activity over complete time course	no
time2QuarterMaxIntegral *(time to ¼ activity)*	Time until quarter of the total cumulative positive activity is passed	yes
time2HalfMaxIntegral *(time to ½ activity)*	Time until half of the total cumulative positive activity is passed	yes
time2ThreeQuarterMaxIntegral	Time until three-quarter of the total cumulative positive activity is passed	yes
max_fold_change	Maximum ratio between the time series and baseline average	no
Total = 190 features		**Total = 71 features**

Table S4: SHAP Values

Average SHAP values (summed over all ligand classes) for top 20 features obtained for XGBoost models trained using all 71 trajectory features from individual and all polarization states. Mean value and corresponding 95% confidence interval is reported from sampling and training the models 15 times.

Feature Name	**Sum of Mean Absolute Values**	**Feature Name**	**Sum of Mean Absolute Values**	**Feature Name**	**Sum of Mean Absolute Values**
M0		**M:IFNβ**		**M:IFNg**	
derivatives_1	2.29±0.07	derivatives_3	1.57±0.07	derivatives_3	2.29±0.08
time_series_2	2.26±0.05	derivatives_1	1.31±0.06	time_series_2	1.77±0.05
derivatives_3	1.85±0.07	intwin0_5_1	1.23±0.10	derivatives_2	1.67±0.12
derivatives_2	1.44±0.07	timeUp2halfMax	1.04±0.07	derivatvies_1	1.34±0.07
timeUp2halfMax	1.43±0.07	time_series_2	0.88±0.04	derivatives_4	0.68±0.05
intwin0_5_2	1.03±0.09	derivatives_4	0.83±0.10	oscpower	0.60±0.03
oscpower	0.97±0.05	derivatives_2	0.80±0.05	timeUp2halfMax	0.60±0.05
intwin0_5_1	0.91±0.12	intwin0_5_3	0.70±0.05	min_amplitude	0.59±0.05
min_amplitude	0.78±0.07	range	0.67±0.05	intwin0_5_2	0.57±0.05
derivatives_4	0.77±0.05	phase_diff1	0.67±0.05	intwin0_5_1	0.55±0.10
range	0.63±0.05	max_pk1_speed	0.66±0.05	range	0.54±0.03
time_series_1	0.60±0.04	maxAmp_early	0.57±0.07	peak_duration_1	0.53±0.05
time2QuaterMaxIntegral	0.58±0.06	min_amplitude	0.54±0.06	max_pk1_speed	0.46±0.04
time2Max	0.56±0.03	time2Max	0.51±0.06	derivatives_11	0.44±0.03
max_pk1_speed	0.56±0.06	derivatives_8	0.51±0.04	derivatives_8	0.42±0.04
maxAmp_early	0.52±0.05	pk1_time	0.50±0.05	maxAmp_early	0.42±0.04

duration_2	0.51±0.04	derivatives_9	0.46±0.04	derivatives_7	0.42±0.05
intwin0_5_3	0.47±0.03	derivatives_10	0.43±0.03	derivatives_5	0.41±0.03
derivatives_8	0.45±0.04	derivatives_5	0.43±0.04	time_series_1	0.40±0.03
intwin0_5_16	0.44±0.04	pk1_prom	0.42±0.04	derivatives_9	0.39±0.04
M:IL10		**M:IL13**		**M:IL4**	
timeUp2halfMax	1.80±0.07	time_series_2	1.57±0.06	derivatives_1	1.66±0.06
time_series_2	1.63±0.05	maxAmp_early	1.31±0.07	maxAmp_early	1.04±0.07
derivatives_1	1.56±0.07	min_amplitude	1.26±0.08	time_series_2	0.91±0.06
derivatives_2	1.09±0.10	derivatives_1	1.18±0.04	range	0.89±0.04
derivatives_3	1.01±0.06	derivatives_3	1.17±0.07	min_amplitude	0.85±0.05
intwin0_5_2	0.88±0.06	derivatives_2	1.07±0.06	pk1_prom	0.79±0.07
intwin0_5_1	0.84±0.11	intwin0_5_2	0.92±0.06	derivatives_3	0.72±0.06
min_amplitude	0.70±0.05	time2Max	0.62±0.05	intwin0_5_1	0.71±0.08
oscpower	0.60±0.06	range	0.60±0.05	derivatvies_4	0.65±0.05
max_pk1_speed	0.57±0.08	intwin0_5_1	0.58±0.06	derivatives_2	0.61±0.06
derivatives_4	0.55±0.04	derivatives_4	0.56±0.05	oscpower	0.58±0.04
max_pk1_speed_frame	0.52±0.05	pk1_times	0.54±0.03	time2Max	0.56±0.06
time2Max	0.48±0.03	timeUp2halfMax	0.52±0.05	max_pk1_speed	0.55±0.04
range	0.43±0.04	max_pk1_speed	0.50±0.04	timeUp2halfMax	0.55±0.06
maxAmp_early	0.43±0.04	derivatives_8	0.49±0.04	pk1_time	0.53±0.07
intwin0_5_3	0.42±0.03	peak_duration_1	0.45±0.06	derivatvies_5	0.40±0.04
pk1_prom	0.42±0.05	time_series_1	0.43±0.03	intwin0_5_2	0.40±0.06
time2QuarterMaxIntegral	0.42±0.04	pk1_width	0.42±0.06	time2HalfMaxIntegral	0.39±0.04

time_series_1	0.41±0.04	derivatives_7	0.41±0.04	derivatives_11	0.38±0.03
derivatives_9	0.41±0.04	oscpower	0.39±0.05	derivatvies_7	0.37±0.05
All					
time_series_2	1.61±0.03				
derivatives_1	1.49±0.04				
derivatives_3	1.43±0.03				
maxAmp_early	1.41±0.06				
intwin0_5_1	1.16±0.05				
min_amplitude	1.15±0.04				
timeUp2halfMax	0.97±0.03				
derivatives_2	0.89±0.03				
intwin0_5_2	0.87±0.06				
intwin0_5_3	0.71±0.06				
derivatives_4	0.58±0.03				
timeDown2halfMax	0.54±0.04				
range	0.53±0.03				
pk1_time	0.52±0.03				
intwin3_1	0.50±0.06				
max_pk1_speed	0.50±0.02				
max_pk1_speed_frame	0.45±0.02				
phase_diff1	0.44±0.02				
time2ThreeQuarterMaxIntegral	0.44±0.03				
peak_duration_1	0.43±0.02				

Table S5: Selected Features

Names of selected features for each polarization condition that were obtained from a recursive feature elimination strategy. For each polarization state, the top 20 features were identified using SHAP analysis on an XGBoost classifier model trained on the task of the discriminating ligand identity. These features were utilized as the starting point for the search strategy and resulted in 6-7 features per polarization state.

	M0	**M:IFNβ**	**M:IFNγ**	**M:IL10**	**M:IL13**	**M:IL4**
Early Activation Speed (EAS)	Derivative – 5min	Derivative – 5min	Derivative – 5min	Derivative – 5min	Derivative – 5min	Derivative – 5min
	Derivative – 10min	Derivative – 20min	Derivative – 15min	Derivative – 15min	Derivative – 15min	Derivative – 15min
			Derivative – 20min			
Peak Activation Speed (PAS)	Time to Max	Time to Max		Time to Max		Time to Max
		Max Derivative to 1st Peak				
Late Activation Speed (LAS)		Derivative – 50min	Derivative – 35min			
Range of Amplitudes (ROA)		1st peak prominence	Range	Minimum Amplitude	Minimum Amplitude	Range
			Amplitude – 5min	Amplitude – 5min	Amplitude – 5min	
Early Phase Activity (EPA)	Integral – 0.5-1hr	1st vs 2nd hr integral			Integral – 0.5-1hr	Integral – 0.5-1hr
Duration (DUR)	Time to ¼ Activity		Duration > 50% Peak	Time to ¼ Activity	Duration > 50% Peak	Time to ½ Activity
Oscillations (OSC)	Oscpower			Oscpower		

Table S6: SHAP Values

Average SHAP values (summed over all polarization classes) for top 20 features obtained for XGBoost models trained using all 71 trajectory features from all stimulation conditions. Mean value and corresponding 95% confidence interval is reported from sampling and training the models 15 times.

Feature Name	**Sum of Mean Absolute Values**
oscpower	0.89±0.02
peak_duration_1	0.53±0.02
min_amplitude	0.48±0.02
timeDown2halfMax	0.44±0.03
derivatives_2	0.41±0.02
derivatives_1	0.39±0.01
maxAmp_early	0.39±0.02
range	0.39±0.01
time_series_2	0.33±0.01
derivatives_3	0.30±0.01
derivatives_4	0.29±0.01
intwin0_5_1	0.29±0.01
duration_2	0.28±0.03
intwin0_5_6	0.28±0.02
intwin0_5_2	0.26±0.01
intwin0_5_3	0.24±0.01
intiwin0_5_7	0.23±0.02
intwin0_5_8	0.23±0.03
duration_1	0.23±0.02
derivatives_25	0.22±0.01